Available online at www.CivileJournal.org

Civil Engineering Journal

(E-ISSN: 2476-3055; ISSN: 2676-6957)

Vol. 10, No. 12, December, 2024

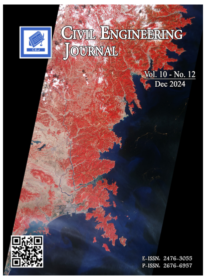

Flood Hazard Assessment Due to Changes in Land Use and Cover

Maman Supratman [1*], Muhammad S. B. Kusuma [2], Muhammad Cahyono [3, 4], Arno Adi Kuntoro [2]

[1] *Civil Engineering Doctoral Program, Faculty of Civil and Environmental Engineering, Bandung Institute of Technology (ITB), Bandung 40132, West Java, Indonesia.*

[2] *Water Resources Engineering Research Group, Faculty of Civil and Environmental Engineering, Bandung Institute of Technology (ITB), Bandung 40132, Indonesia.*

[3] *Civil Engineering Department, Faculty of Engineering and Sciences, Ibnu Khaldun Bogor University, Kota Bogor 16162, Indonesia.*

[4] *Center for Ecohydrology, Ecohydraulics and Engineering Science, Bandung 40132, Indonesia.*

Received 12 June 2024; Revised 24 October 2024; Accepted 06 November 2024; Published 01 December 2024

Abstract

This study aimed to investigate the influence of land use changes on the occurrence of flood hazards in the Pondok Karya area, Jakarta, Indonesia. Landsat OLI 8 and 7 from 2002 to 2023 were analyzed with a supervised classification tool using Envi and ArcGIS to investigate land use changes over the period. Additionally, the HEC-HMS and HEC-RAS tools were utilized for hydrological and hydraulic assessments under 25 discharge return periods (Q25), using a daily rainfall dataset from 2004 to 2021. The flood hazard index was produced using statistical and GIS methodologies and was based on Neighbourhood Associations (NAs) after qualified hydraulic model performance, indicating a Nash 0.65–Nash-Sutcliffe model efficiency (NSE) value. The analysis revealed considerable alterations in land use and cover within the Pondok Karya watershed. Consequently, the percentage of urban areas surged 30%, whereas vegetative cover declined 24%. Additionally, bare land decreased 9%, and water bodies marginally increased 3%. This indicates a 10% increase in the peak flood river flow of Mampang, from approximately 90 m³/s to 100 m³/s within this period. Subsequently, the percentage of high-risk areas increased from 42.85% (six NAs) to 57.14% (eight NAs), whereas the percentage of low-risk areas decreased from 14.29% (two NAs) to 7.14% (one NAs). Moderate-risk areas also decreased from 42.85% (six NAs) to 35.71% (five NAs). The study found that despite vegetative cover exceeding 30%, the capacity of the Mampang River remained inadequate, and the risk of flooding increased with the impact of its conversion. Additionally, the soil properties and social intervention factors contributed to the performance of the inundation model. Our study underscores the need for further research to mitigate flood risks and advocate interventions such as reservoir construction or river normalization in the upper Mampang catchment area. This study is useful for both local and central governments, which act as decision-makers to reduce the risk of flooding.

Keywords: Land Use Change; HEC-HMS Model; HEC-RAS Model; Q25 Flood Design; Flood Hazards Index.

1. Introduction

Jakarta is a low-lying metropolitan area prone to river flooding, as indicated by studies conducted by Wijayanti et al. [1] and Budiyono et al. [2]. The risk of flooding has heightened due to rapid urbanization, changes in land use and land cover (LULC), and deforestation [3-5]. The conversion of green open spaces to urban areas in cities has led to an increase in surface runoff in drainage systems and river discharge in the main channel [6-9].

* Corresponding author: ms120485@gmail.com; 35021014@mahasiswa.itb.ac.id

http://dx.doi.org/10.28991/CEJ-2024-010-12-04

Furthermore, global climate change contributes to an increase in the frequency of extreme rainfall events, resulting in increased vulnerability of areas to flooding owing to inadequate drainage capacity [10, 11]. Socioeconomic growth is the primary catalyst for land-use changes that affect ecosystem services. The change in LULC has resulted in the elevation of the land surface and air temperature within urban areas [12, 13]. Furthermore, this change has the potential to amplify the risk of disasters and exacerbate the effects of global environmental changes [14, 15]. It has the potential to elevate the danger of flooding by generating a significant surge in water flow in the future [16, 17]. The transformation of land use in Jakarta has occurred gradually and is primarily influenced by increasing population concentration [18]. In addition, the urban region encompassing Jakarta, Tangerang, Bogor, Depok, and Bekasi experienced substantial transformation, amounting to approximately 70% of the area over 20 years from 2001 to 2021 [19].

Pondok Karya, located on relatively flat terrain in South Jakarta, is prone to flooding during periods of rainfall. Historical data suggest that the flood typology is characterized by a combination of fluvial and pluvial flooding [20]. The population density in this area is approximately 18,000 individuals per square kilometer, with an average temperature of 27 °C. The humidity ranged from 80% to 90%, and the average annual rainfall was approximately 2600 mm. The region spans approximately 10 ha and is divided into 14 Rukun Tetangga (RT) or Neighbourhood Associations (NAs). From a hydrological perspective, this area is situated in the lower section of the Mampang sub-watershed, downstream of the Krukut Watershed. The river is an urban transboundary waterway, with a catchment area of approximately 88.50 km². The Mampang catchment area, which accounts for 41.80% of the overall Krukut catchment area, covers approximately 37 km². The Krukut outflow is influenced by the discharge of the Ciliwung River, which is located within the Ciliwung-Cisadane River Basin. This means that the likelihood of flooding in Krukut is directly affected by coastal flooding in downstream areas, such as the Muara Angke West Canal flood [24].

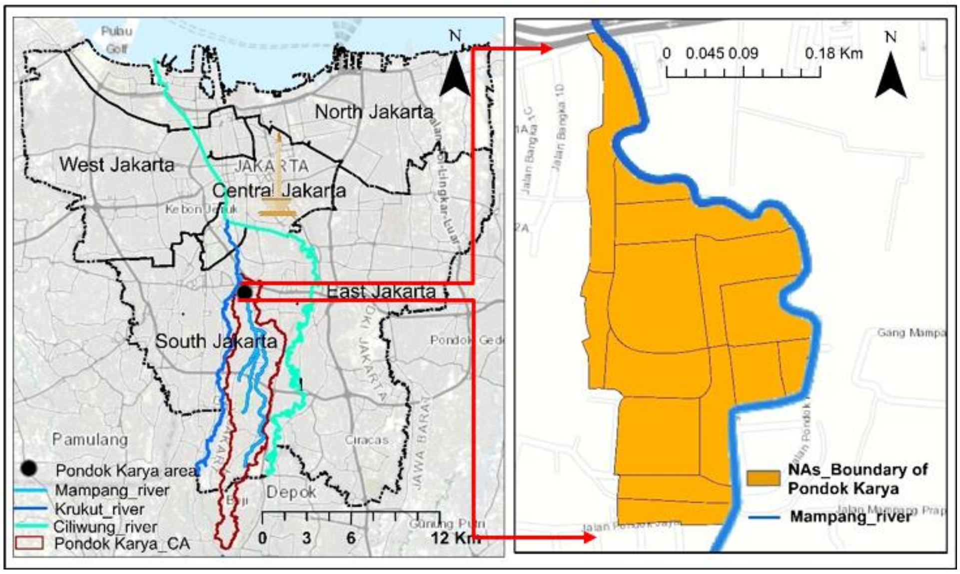

Figure 1. Pondok Karya region and its catchment area, Jakarta Indonesia

The risk of flooding can be effectively reduced in Kemang and Pondok Karya by harnessing the power of a retarding basin or an artificially constructed wetland as a nature-based solution (NbS) covering an area of approximately 10 ha. Local authorities have asserted that such interventions can diminish peak flooding by approximately 20% in the downstream stretch of the Krukut River during intense rainfall, registering 200 mm/day. Beyond its primary function of floodwater storage during peak periods, the implementation of NbS offers a multifaceted array of benefits. They can double as public spaces based on green infrastructure, catering to the recreational and sporting needs of citizens. NbS has also been recognized as a global strategy for addressing climate change, with the potential to enhance urban resilience [22-25].

Yosua et al. (2024) showed that urban flooding in South Jakarta stems from shifts in LULC, resulting in an increased risk of pluvial hazards. According to Taufik et al. (2022), implementing river normalization measures along the Bendungan Hilir stretch holds promise for substantially mitigating flood hazards, potentially reducing risks by 75% for a Q25 return period. Furthermore, the Kemang area stands identified as a high-risk flood zone, evidenced by its susceptibility to inundation during a 2-year rainfall return period, with recorded depths reaching 1.5 m in 2020 [26]. This flooding, which is a confluence of natural forces and socioeconomic factors, underscores the need for proactive measures to mitigate flood risks [27]. The occurrence of intense rainfall events in this region is driven by global climate change [6, 28]. Low-impact development (LID) techniques, such as rain gardens, rainwater harvesting, and permeable pavements, can be efficient options for lowering surface runoff at the watershed level while also being cost-effective [29, 30].

Flood hazards commonly increase owing to land use and land cover changes in Indonesia. Several examples of previous comprehensive flood studies in Indonesia are available for highly developed areas, such as the Bandung Flood [7, 31], Jakarta Flood [20, 32-34], and Solo Flood [35], or new iconic areas for mangrove conservation, such as Langsa City [36]. Most floods are generated by rain runoff, tides, dam-break flows, or a combination of these generators, as discussed in previous studies [7, 20, 31-33, 35, 37-40]. Several flood mitigation measures have been implemented, including river normalization, sluice gates, reservoirs, rainwater harvesting systems, and flood early warning systems (FEWS) [20, 25, 33, 35, 36, 38-44]. However, FEWS appears to be the most effective method for reducing flood risk [31, 42]. Meanwhile, reservoir development has become less favorable owing to the increasing reservoir water quality problems [43] and the increasing trend of earthquakes that can generate dam breaks [14, 15].

Assessing the impact of land use changes on the risk of flooding in urban areas is essential, particularly in Indonesia, where cities are frequently located and built on floodplains. Pondok Karya is a notable case study for evaluating the likelihood of flooding and for implementing suitable measures to mitigate this risk. The anticipated outcome of this study has the potential to bridge the existing gap and serve as a valuable reference for local governments in formulating strategies and programs in the future. Pondok Karya is a flood-prone area with flat areas and swamps along the Krukut River. Currently, floods generate higher hazards to the surrounding communities, infrastructure, and lifelines in Pondok Karya. However, a comprehensive study of flood hazards in Pondok Karya has not yet been conducted. Therefore, this study presents the results of a flood hazard study.

2. Materials and Methods

2.1. Materials

This study utilized DEMNAS topographic satellite imagery data from the Indonesian Geospatial Agency (Badan Informasi Geospatial or BIG), accessed at *https://tanahair.indonesia.go.id/portal-web/*. The data had a spatial resolution of 8 × 8 m and were utilized to delineate the boundaries of the Krukut watershed. Subsequently, to examine LULC alterations, images from the Landsat OLI 7 and -8 satellites spanning 2002 to 2023 were acquired from *https://earthexplorer.usgs.gov/*. The images had a grid size of 30 × 30 m. Daily precipitation data collected from rain gauge stations encircling Jakarta from 2004 to 2021 were obtained from the Indonesian Meteorological and Geophysics Agency (Badan Meteorologi, Klimatologi, dan Geofisika, or BMKG) and Jakarta's Water Resources Agency (Dinas Sumber Daya Air Jakarta or DSDA Jakarta).

Using the Thiessen Polygon method, the spatial rainfall data gathered from these stations were analysed. The drainage network, initially derived from DEMNAS satellite imagery, was validated using field data. River geometry data were sourced from DSDA Jakarta, while inundation data from 2016 to 2023 served the dual purpose of validating the hydraulic model. The hydrological soil group and curve number were determined using soil data, infiltration rates, and geological features obtained from DSDA Jakarta. The global hydrological soil group map was sourced from *https://daac.ornl.gov/SOILS/guides/Global_Hydrologic_Soil_Group.html*.

2.2. Methods

DEMNAS topographic data were used to delineate the boundary of the Krukut watershed using hydrological spatial analysis tools in ArcGIS. These tools include fill, flow direction, flow accumulation, stream-to-order, stream feature, and snap-pour points. Subsequently, to generate sub-catchment boundaries for Pondok Karya, the HEC-HMS software was employed in conjunction with GIS features. This process includes tools for terrain reconstruction, sink preprocessing, drainage preprocessing, stream identification, breakpoint management, and delineation. Figure 1 shows the flowchart of the research methodology through which the objectives of this study were achieved.

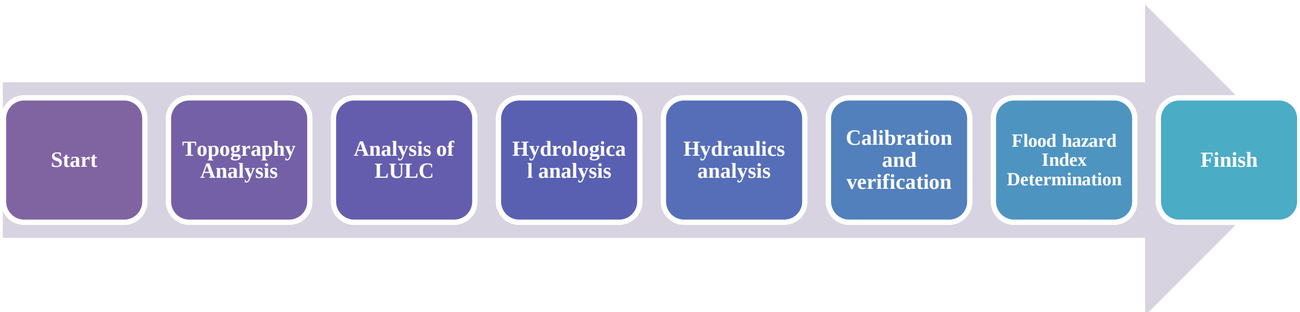

Figure 2. Research framework

A supervised classification (maximum likelihood) method was executed using Envi and ArcGIS to analyze the LULC changes within the Pondok Karya catchment area from 2002 to 2023. The number of samples in each class was approximately 20–30 samples. This method categorizes LULC into four distinct classes: water bodies, vegetation, urban areas, and barren land. The resulting analysis determined the proportion of impervious areas in each subcatchment as represented by the curve number. These were necessary for subsequent hydrological analyses using the HEC-HMS software. HEC-HMS and HEC-RAS coupled models have been extensively used in studies for assessing rainfall-runoff and inundation simulations in a variety of geographical situations, including river basins and small urban areas [45-47].

In addition, the frequency and distribution of rainfall were assessed using historical daily rainfall data. The rainfall return periods for Q25 and Q50 were calculated using rainfall intensity data. The hydraulic system was simulated in the HEC-RAS using the discharge data obtained from the HEC-HMS. Losses were computed in the HEC-HMS using the Soil Conservation Service (SCS) curve number (CN) approach, and the data were transformed using the SCS unit hydrograph method, assuming the absence of baseflow. The rainfall runoff was estimated using the following equation:

$$Q = \frac{(P - I_a)^2}{(P - I_a) + S} \tag{1}$$

where Q is the runoff (in), P is the rainfall (in), I_a is the initial abstraction (in), and S is the potential maximum retention after runoff begins (in).

$$I_a = 0.2S \tag{2}$$

$$Q = \frac{(P - 0.2S)^2}{(P + 0.8S)} \tag{3}$$

$$S = \frac{1000}{CN} - 10 \tag{4}$$

The hydraulic simulation was conducted in a 1D format and then in a 2D model following successful execution. Hydrological and hydraulic analyses were conducted under two distinct scenarios: pre- and post-LULC alteration. The hydraulic 1D model was then calibrated using historical flood event data. This was assessed using Nash-Sutcliffe Efficiency (NSE) values. If the value is closer to 1, the NSE value is better and vice versa (Table 1). Model verification was carried out by conducting field surveys and interviews with local residents of the research area.

$$NSE = 1 - \frac{\sum_{i=1}^{N}(X_i - Y_i)^2}{(X_i - \overline{X}_i)^2} \tag{5}$$

where X_i is observed data, Y_i is simulated data, X_i is average observed data, N is the number of data.

Table 1. Criteria of Nash-Sutcliffe Efficiency (NSE) Value

NSE Value	Interpretation
NSE > 0.75	Good
0.36 < NSE < 0.75	Qualified
NSE<0.36	Not Qualified

These scenarios were designed to assess the flood hazard index (FHI) in the Pondok area before and after the developmental phase, specifically during the Q25 return period (Table 2).

Table 2. Hazard index criterion

Inundation Depth				
Depth (cm)	**Class**	**Rate**	**Weight (%)**	**Score**
<76	Low	1		0.4
76–150	Moderate	2	40	0,8
>150	High	3		1.2
Duration of Inundation				
Duration (hour)	**Class**	**Rate**	**Weight (%)**	**Score**
< 12	Low	1		0.2
12–24	Moderate	2	20	0.4
> 24	High	3		0.6
Inundation Area				
Area (m^2)	**Class**	**Rate**	**Weight (%)**	**Score**
< 100	Low	1		0.2
100–300	Moderate	2	20	0.4
>300	High	3		0.6

Inundation Frequency				
The number of events	**Class**	**Rate**	**Weight (%)**	**Score**
0–5	Low	1		0.2
6–20	Moderate	2	20	0.4
> 20	High	3		0.6

The Flood Hazard Index (FHI) was calculated using the following Equation:

$$FHI = 0.4 \text{ score of flood depth} + 0.2 \text{ score of flood duration} + 0.2 \text{ score of inundation area} + 0.2 \text{ score of inundation frequency} \tag{6}$$

This criterion was derived from the Indonesian National Disaster Mitigation Agency (Badan Nasional Penanggulangan Bencana) and the Ministry of Public Works (PUPR). The criteria consisted of four indicators: inundation depth (cm), length (h), size (m^2), and frequency of inundation. The FHI is a component of the flood hazard parameters, whereas the others are vulnerability and capacity indices.

3. Results and Discussion

3.1. Digital Elevation Model

The digital elevation model used in this study was obtained from the BIG website. The watershed boundaries of Krukut and Mampang were demarcated using a hydrological spatial analysis tool, as shown in Figure 3. The catchment basin of the river spans approximately 89 km², and the mainstream measures more than 30 km in length. This model was instrumental in defining the boundary of sub-catchments and drainage networks using the Geographic Information System (GIS) component of the HEC-HMS software. A total of 26 sub-catchments were identified, with 17 specifically allocated to Mampang, covering an area of approximately 37 km², equivalent to approximately 41% of the Krukut watershed. Subsequently, Pondok Karya was situated in the Mampang Hilir sub-watershed, with a total area of 3.11 km², encompassing 14 Neighborhood Associations (NAs).

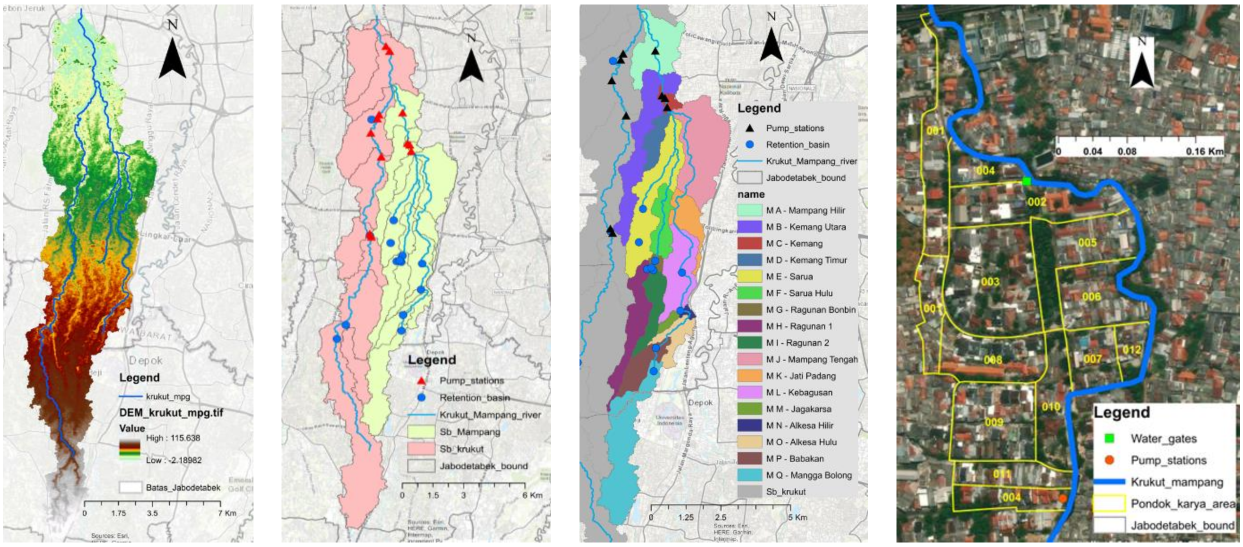

Figure 3. Digital elevation model (left), Krukut and Mampang watershed boundaries (centre), and Pondok Karya area (right)

Satellite images of Landsat OLI 8 and -7 with a spatial resolution of 30 × 30 m were extracted from online sources at https://landsat.gsfc.nasa.gov/satellites/landsat-8/ for 2002 to 2023. The dataset was then corrected with radiometric and geometric data using a ground control point (GCP) and digital elevation DEM to relieve the displacement corrected by the data provider before it was distributed. Classification was performed using Landsat 7 (2002–2013) and 8 (2018–2023) image data at the L1TP level. However, with Landsat 7 images, a gap-filling procedure is required to fill pixel gaps. ENVI software was used for classification processing. Next, a natural color composite channel selection (band 4-3-2) was used for visual interpretation. Class selection was based on the requirements of the land cover analysis and most cover classes, which were then defined as polygons for each class to serve as training samples. Maximum Likelihood was used for the supervised categorization [48]. However, for accuracy testing, additional polygons that differ from the training samples must be defined. The classification findings, once collected and meeting the Overall Accuracy calculation value, were used for further investigation. The average accuracy was 80.71%, which suggests that it is within the acceptable range, where the minimum acceptable accuracy is above 75% [49].

As depicted in Figure 4, significant LULC alterations occurred in the Mampang sub-watershed during the 20-year study period. In 2002, urban areas accounted for approximately 55% of the total area, vegetation covered 34%, bare land occupied 10%, and aquatic bodies accounted for the remaining 1%. Notably, the vegetative region was predominant in the upstream and middle sections of the Pondok Karya catchment. Substantial urban development has transformed the landscape, with urban areas accounting for 74% of the total, vegetation declining to 12%, bare land experiencing a modest increase to 11%, and aquatic bodies climbing to 3%. By 2023, the urban area will cover approximately 85% of the Mampang sub-watershed, whereas vegetation, water bodies, and bare land will account for 10%, 4%, and 1%, respectively. Notably, the map revealed a substantial conversion of bare land to urban areas, accounting for approximately 10% of the total area. The percentage of urban areas in Pondok Karya will experience a significant and rapid increase from 2002 to 2023, reaching almost 30%. Conversely, there was a decrease of approximately 24% in the vegetation percentage during the same period. Furthermore, the percentage of bare land decreased from approximately 10% to 1%, whereas the percentage of water bodies exhibited a modest increase from 1% to 4%.

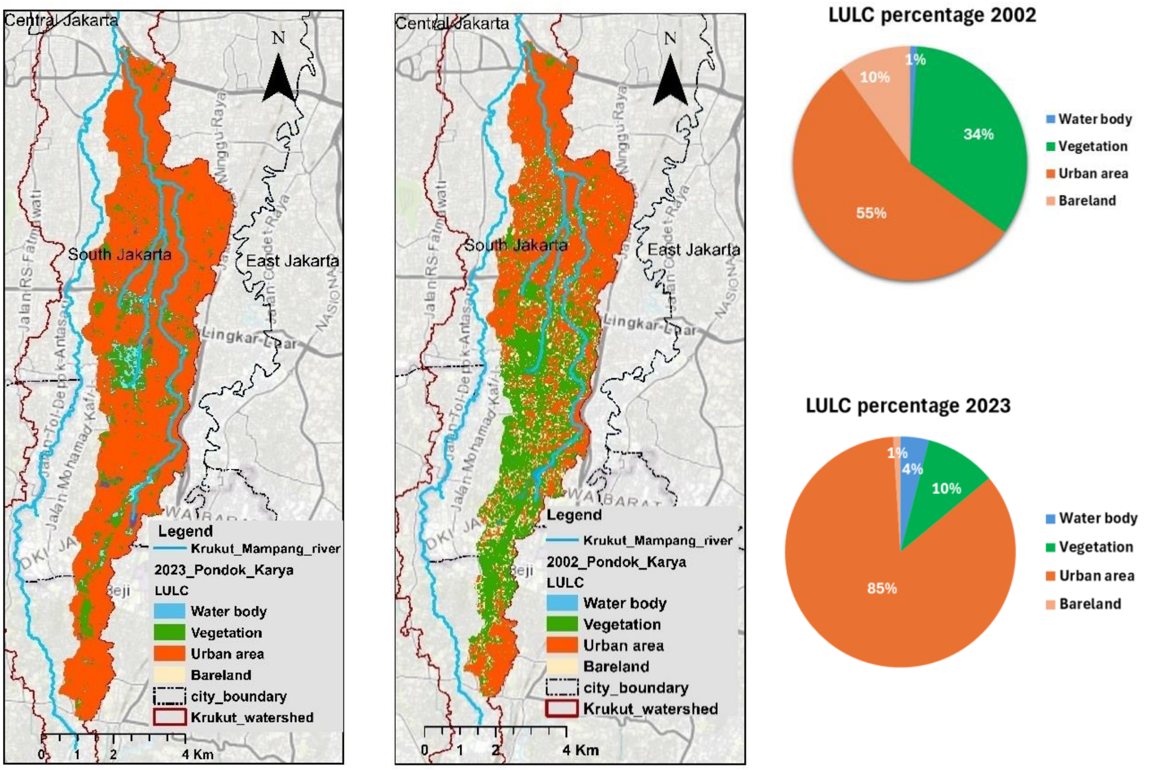

Figure 4. LULC percentage during 2002 (left) and 2023 (right)

Changes in land use and land cover changed the curve number over the 17 sub-basins in the Mampang watershed. This alteration in impervious areas could be indirectly associated with changes in surface runoff for each sub-catchment of the Pondok Karya region. This phenomenon can be found more in the upper part of the sub-basins, such as Alkesa Hilar, Jati Padang, Kebagusan, Mampang Tengah, and Sarua, which experienced increased CN values of 5.14%, 9.52%, and 4.35%, respectively, which is closely related to an increase in the percentage of impervious surfaces in this region. The lower part of the sub-basin, such as the Mampang Hilir, has a relatively small change in CN compared with the upper region because this area was detected to have become urban (Table 3).

3.2. Soil, Infiltration Rate, and Geological Properties

Based on the collected data, the Mampang sub-watershed was categorised into two geological formations: alluvium and alluvium fans. This classification indicates a low water infiltration rate and limited capacity to hold water within the area. The water table depth in the Mampang sub-watershed ranged from 2 to 38 m, with the highest recorded infiltration rate being 1.64 mm/h, reflecting remarkably low infiltration capabilities. This results in the generation of significant surface runoff during rainfall periods (Figure 5).

Table 3. Impervious areas of sub-basins over the Pondok Karya catchment area

Sub-basin name	Area (km^2)	Total Area (%)	Impervious Area in 2002 (%)	Curve Number in 2002	Impervious Area in 2023 (%)	Curve Number in 2023
M Q - Mangga Bolong	5.17	13.94	38.69	93.17	85.26	92.87
M P - Babakan	1.52	4.09	6.69	91.57	67.16	91.37
M D - Kemang Timur	1.05	2.82	71.11	90.58	90.56	88.87
M A - Mampang Hilir	3.11	8.38	93.66	90.60	94.31	91.85
M G - Ragunan Bonbin	0.24	0.65	5.03	88.61	5.44	85.63
M H - Ragunan 1	2.48	6.69	16.98	83.63	83.98	71.12
M I - Ragunan 2	1.52	4.11	24.65	70.32	86.27	40.29
M M - Jagakarsa	0.30	0.81	41.08	83.58	95.59	90.40
M C - Kemang	0.42	1.14	68.86	82.47	81.96	89.51
M B - Kemang Utara	4.01	10.82	83.85	88.97	89.58	88.64
M F - Sarua Hulu/Mpg	1.52	4.09	33.94	93.12	52.90	93.52
M E - Sarua	4.58	12.34	57.14	88.00	78.11	89.43
M J - Mampang Tengah	5.30	14.30	86.70	86.06	94.93	91.24
M L - Kebagusan	2.95	7.96	35.99	85.43	86.55	89.15
M K - Jati Padang	1.57	4.23	58.75	86.20	84.44	94.40
M O - Alkesa Hulu	1.18	3.19	46.96	92.64	85.93	93.96
M N - Alkesa Hilir	0.16	0.42	86.63	87.10	94.39	91.58
Total	**37.07**	**100%**				

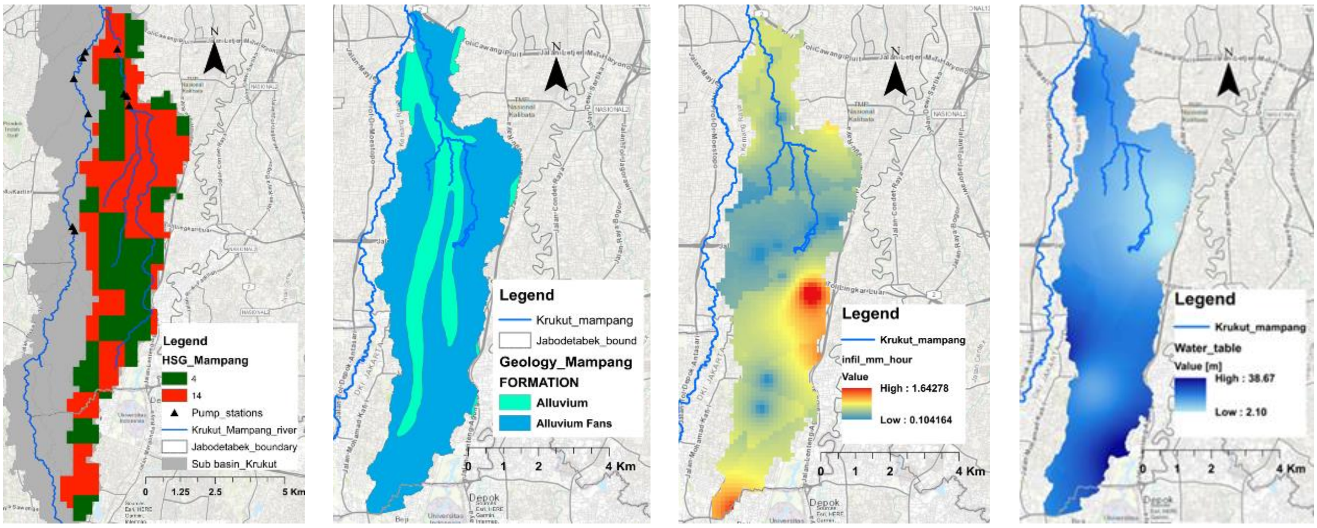

Figure 5. River Mampang discharge for a 25-year return period (Q25)

Based on Global Hydrologic Soil Group (HSGs) data, the area falls within the range of 4 to 14, corresponding to class D. Typically, this classification indicates a composition with more than 40% clay and less than 50% sand, predominantly featuring clay-like textures. The soil analysis report at Jagakarsa revealed that the soil type had a high plasticity index, suggesting a clay-like consistency in the top 5 m below the surface. The plasticity of soil, characterized by high stickiness, indicates significant cohesive forces among clay particles, resulting in adhesiveness [50]. Consequently, this soil type possessed a greater capacity to retain water as surface runoff rather than absorbing it into the soil.

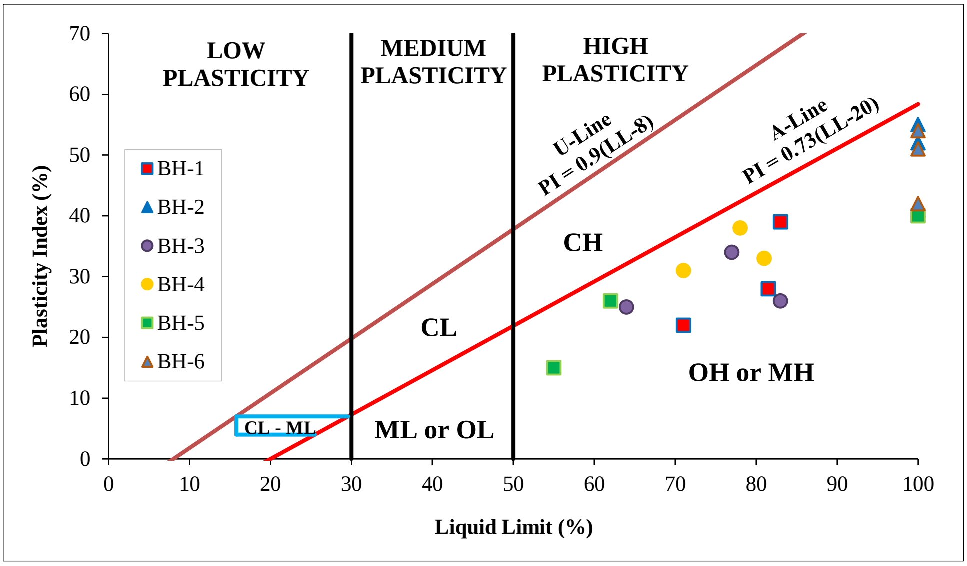

Figure 6. Jagakarsa soil characterization based on liquid limit vs plasticity index

3.3. Rainfall and Inundation

Rainfall and inundation have experienced an upward trajectory owing to global climate change. In January 2020, the rainfall intensity increased to 377 mm/day. Rainfall distribution analysis using Thiessen polygons indicated that Pondok Karya was influenced by the rain gauge stations at Halim Perdana Kusuma, South Tangerang, UI Campus, and Cibinong.

Consistency data for rainfall were checked using a double-mass curve to ensure that the quality of the input data met the standard and to minimize errors in the simulation processes. The results of checking the consistency of the rainfall data are as follows. Rainfall data met the quality data standard, which can be observed by the coefficient correlation value (R), which was closer to 1 for both stations.

Surface runoff and stream discharge were predicted using the HEC-HMS rainfall-runoff model. The anticipated average daily rainfall over a 25-year period was approximately 208 mm/day.

The rainfall trend at the five rain gauge stations increased dramatically over the 18-year period. Inundation depth data were collected from the Water Resources Agency of Jakarta. These data were then compared with daily rainfall data from a rain gauge station in the surrounding area. The inundation depth was observed at three locations: Kemang Utara, Kemang Raya, and Pondok Karya. Several variables contributed to the river's dynamic value, including the spatial distribution of rainfall, the intervention of water gates in Manggarai and Karet by human operators, and the sediment rate and solid waste in the Mampang Channel. These conditions had the ability to diminish the existing river capacity and disrupt the hydraulic function, as illustrated by the graph of rainfall constraint on the inundation pattern in Figure 7. Noticeably, at specific points from September 2016 to 2018, where rainfall was greater than that in August 2016, the inundation depth was less than that in August 2016. This could have occurred because of the large amount of solid trash being disposed of straight into the river, as seen in Figure 4, and many people intervening along the riverfront without the required safe distance. Furthermore, the lack of environmental facilities near the river, such as temporary landfills, wastewater treatment plants, and sewage drainage networks, as well as citizen awareness, causes the river to be converted into a landfill. However, in 2020 and 2021, the inundation pattern coincided with rainfall depth occurrences owing to the local government's well-planned action of river dredging and stationing green troops along the river to manually pick up solid trash on the Mampang River.

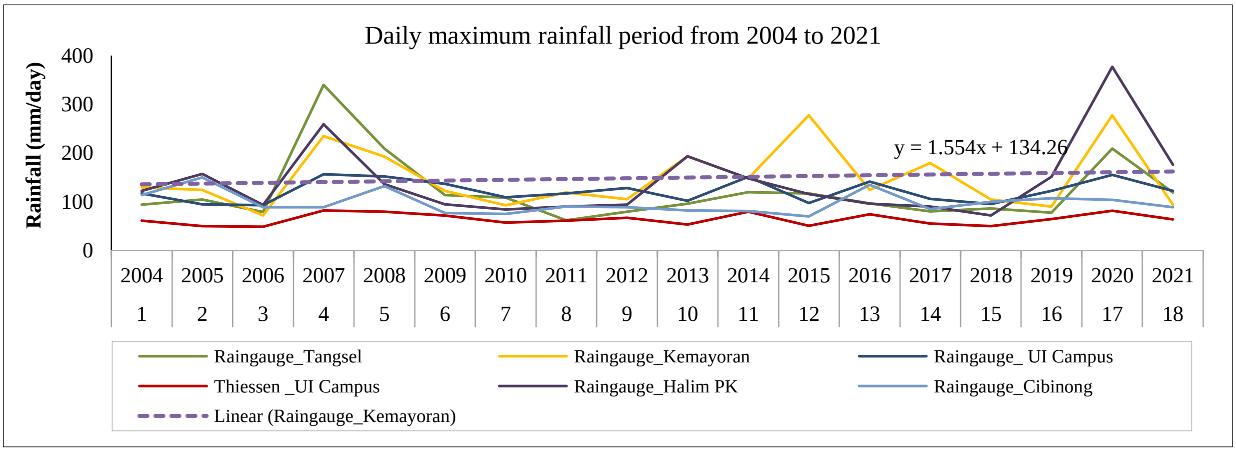

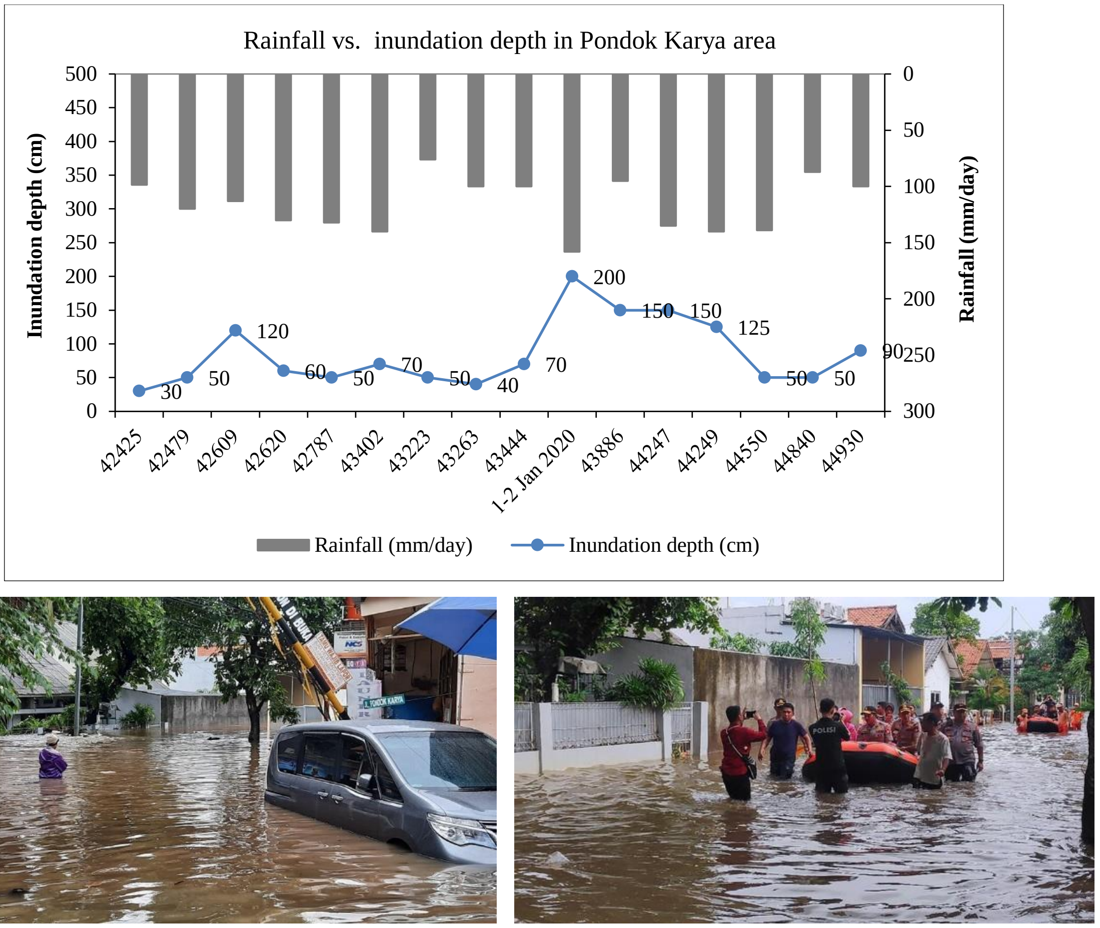

Figure 7. Daily maximum depth of rainfall and inundation events around the Krukut-Mampang watershed

3.4. Hydrologic and Hydraulics Model Setup

The hydrological analysis began with an examination of rainfall patterns, encompassing their distribution and frequency. This study utilized a daily rainfall dataset spanning from 2004 to 2021, as shown in Figure 8.

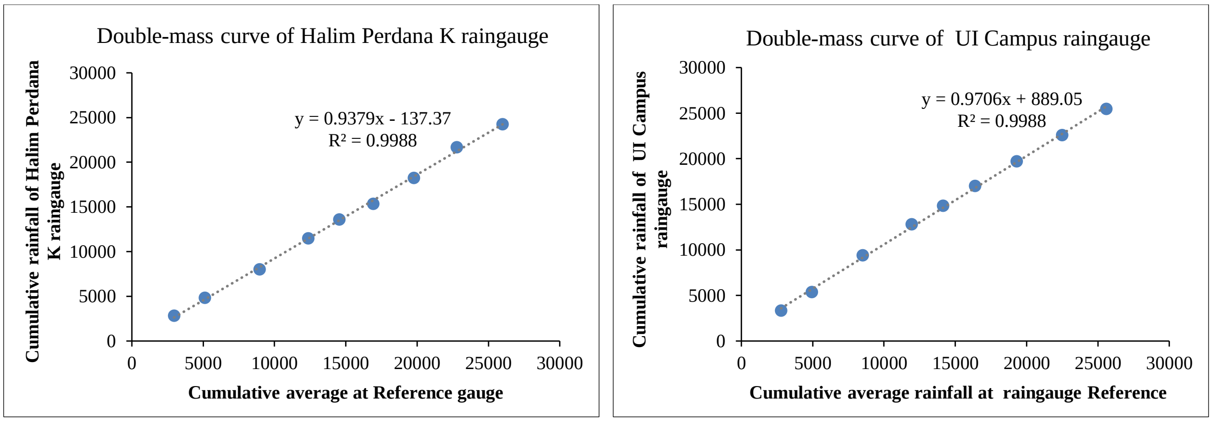

Figure 8. Double mass-curve of Halim Perdana Kusuma and UI Campus rain gauge

In the HEC-HMS, for each subbasin, the Soil Conservation Service (SCS) Curve Number and SCS Unit Hydrograph Model were applied for the loss and transform method. The loss parameters were the initial abstraction, CN, and percentage of impervious surfaces. The Transform parameters were filled by graph type (Delmarva) and lag time, whereas the time-based running was set for 3 days and 18 h, with an interval time of 1 h.

In the hydraulic model, the upstream part was configured with flow hydrographs (Hulu 2, Hulu 3, and Hulu 4) followed by lateral inflow for D1 (Serua sub-basin), D2 (Mampang Hilir sub-basin), B1 (Kemang sub-basin), and B2 (Kemang Utara sub-basin), as depicted in Figure 9. Then, the outflow boundary condition of the Krukut-Mampang was set to the normal depth. The flow simulation was set to unsteady flow, both in 1D and 2D models.

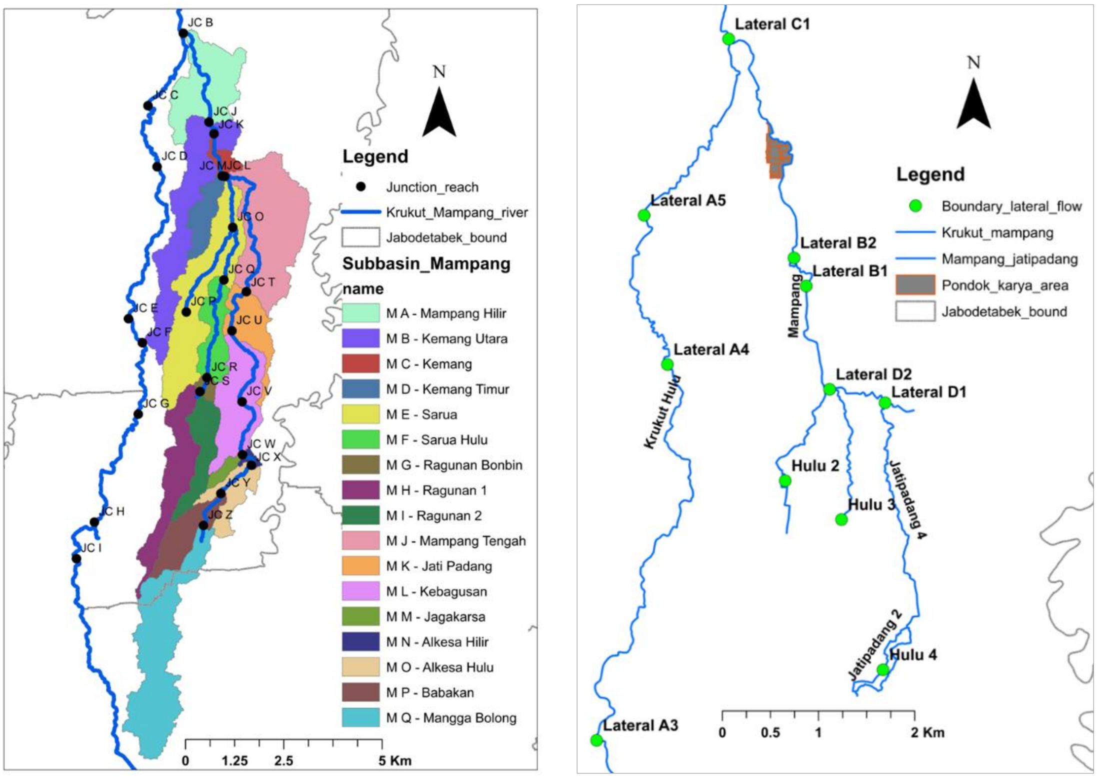

Figure 9. Hydrologic and hydraulic model setup for Pondok Karya

3.5. Hydrologic Model

The model indicated that the peak stream discharge for Q25 in JCO Hulu 3 was approximately 19.50 m^3/s and 15.4 m^3/s, while for JCT Hulu 4; it was approximately 40.2 m^3/s and 35.70 m^3/s for the years 2002 and 2023, respectively. Consequently, there was growth of approximately 26.60% and 12.60% following development. Furthermore, JCT Hulu 4 was released twice as many times as JCO Hulu 3 in response to an effective rainfall flux of approximately 162.8 mm (Figure 10).

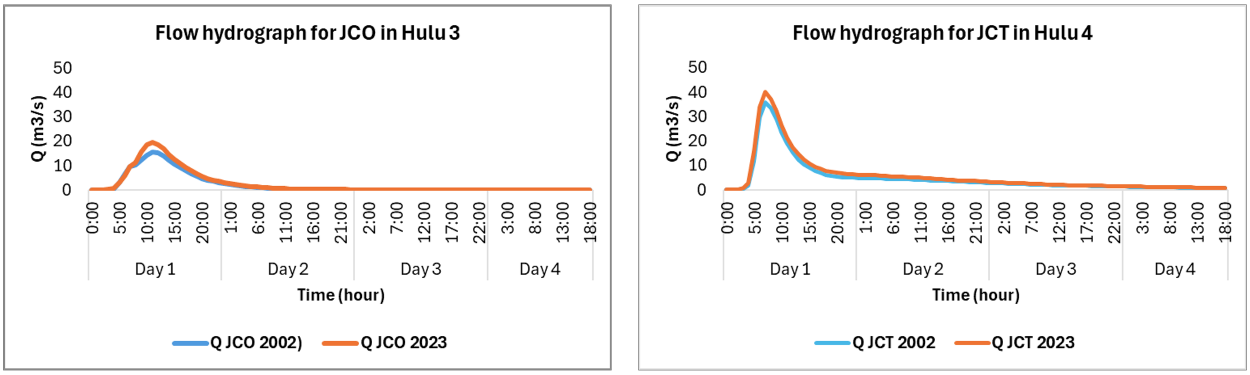

Figure 10. Flow hydrographs in JCT Hulu 3 and Hulu 4 for a 25-year period (Q25)

The peak flood decrease was lower than the percentage change in the vegetation cover, which exceeded 30%. This may be attributed to the soil type and subterranean features of the Mampang Subcatchment. According to the soil data, the area consists mainly of clay and sand, which have a low potential for water infiltration.

The insufficient drainage capacity of JCT Hulu 4, coupled with the need to manage large flood discharges from many catchment areas, led to longer drainage durations compared to JCO Hulu 3. JCO Hulu 3 encompassed multiple subcatchments in the upstream region: Ragunan 1, Ragunan 2, Bonbin, and Mampang. JCT Hulu 4 comprises several sub-catchments, namely, Mangga Bolong, Babakan, Alkesa Hulu, Alkesa Hilir, Jagakarsa, Kebagusan, and Jati Padang, as shown in Figure 9.

As shown in Figure 11, the surface runoff in the Mangga Bolong Sub-basin increased from approximately 20 m^3/s to approximately 25 m^3/s, followed by that in Kebagusan which increased from 15 m^3/s to 18 m^3/s. Similar patterns were observed in other subcatchments such as Ragunan 1 and Ragunan 2. These responses correlate with the proportion of land cover, as shown in Table 3. The Mampang Tengah sub-basin emerged as the highest contributor to the peak flood discharge in the Pondok Karya area at approximately 28 m^3/s, followed by Mangga Bolong, Serua, and Kebagusan at approximately 22 m^3/s, 20 m^3/s, 18 m^3/s, respectively. Mampang Hilir and Kemang Utara exhibited relatively constant discharge levels between 2002 and 2023, hovering at approximately 18 m^3/s.

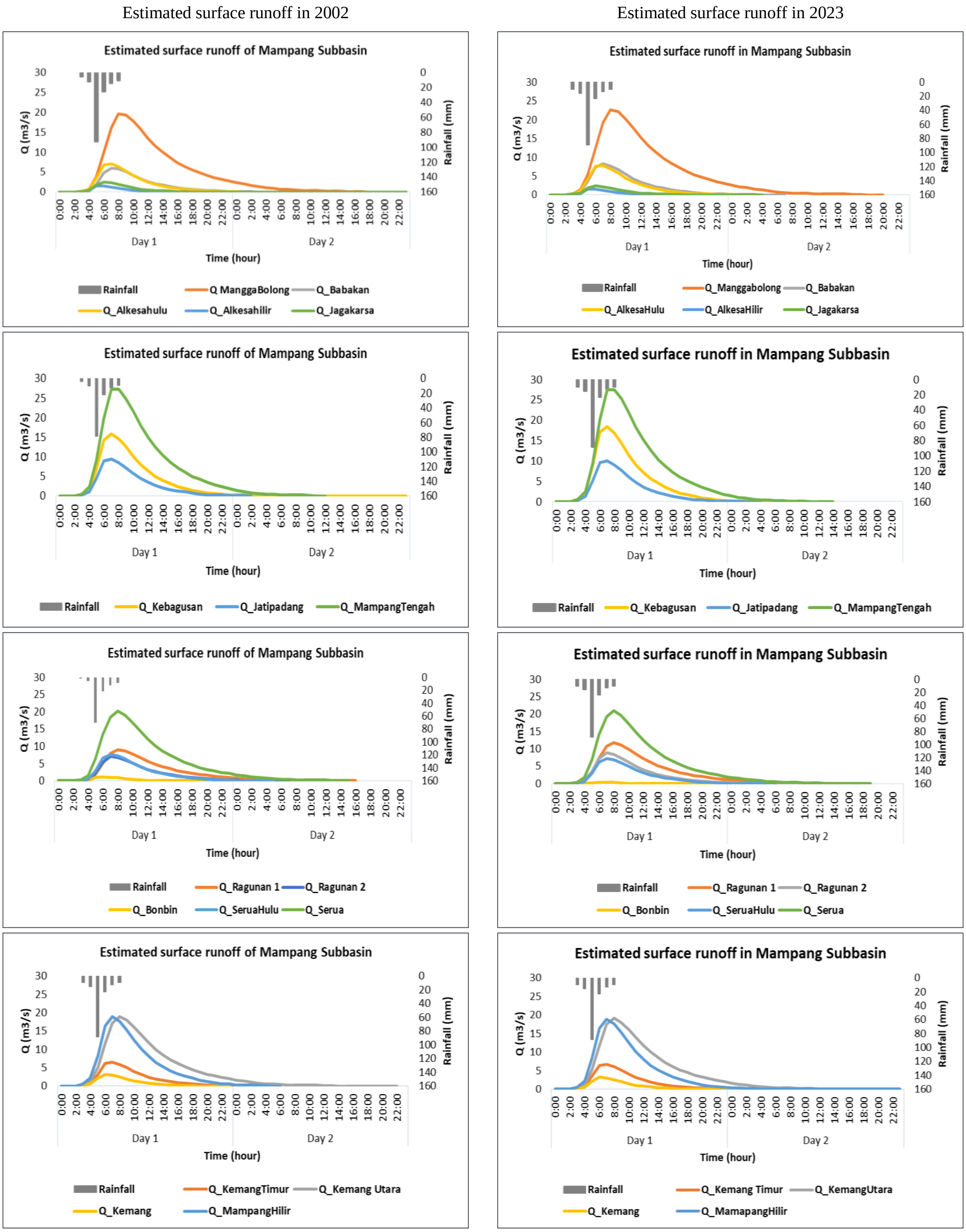

Figure 11. Comparison of estimated surface runoff for each sub-basin for the 25-year period discharge design (Q25)

3.6. Hydraulics Model

The hydraulic analysis of Pondok Karya was conducted using HEC-RAS software, utilizing both 1D and 2D models. The model was designed to comprehensively represent the Krukut Watershed. A hydraulic 1D model was employed to determine the temporal delay of the bankfull stage and quantify the disparity in flood depth between 2002 and 2023. In the 2D model, the cell grid size was set to 10 × 10 m for the 2D flow region and 3 × 3 m for the channel. The study was undertaken during two distinct periods: prior to development in 2002 and after development in 2023. The border conditions of the area upstream of Pondok Karya consist of Hulu 2, Hulu 3, and Hulu 4. The lateral inflow was composed of Jatipadang, lateral D1, D2, B2, and B1. The outflow was adjusted to a normal depth (Figure 12).

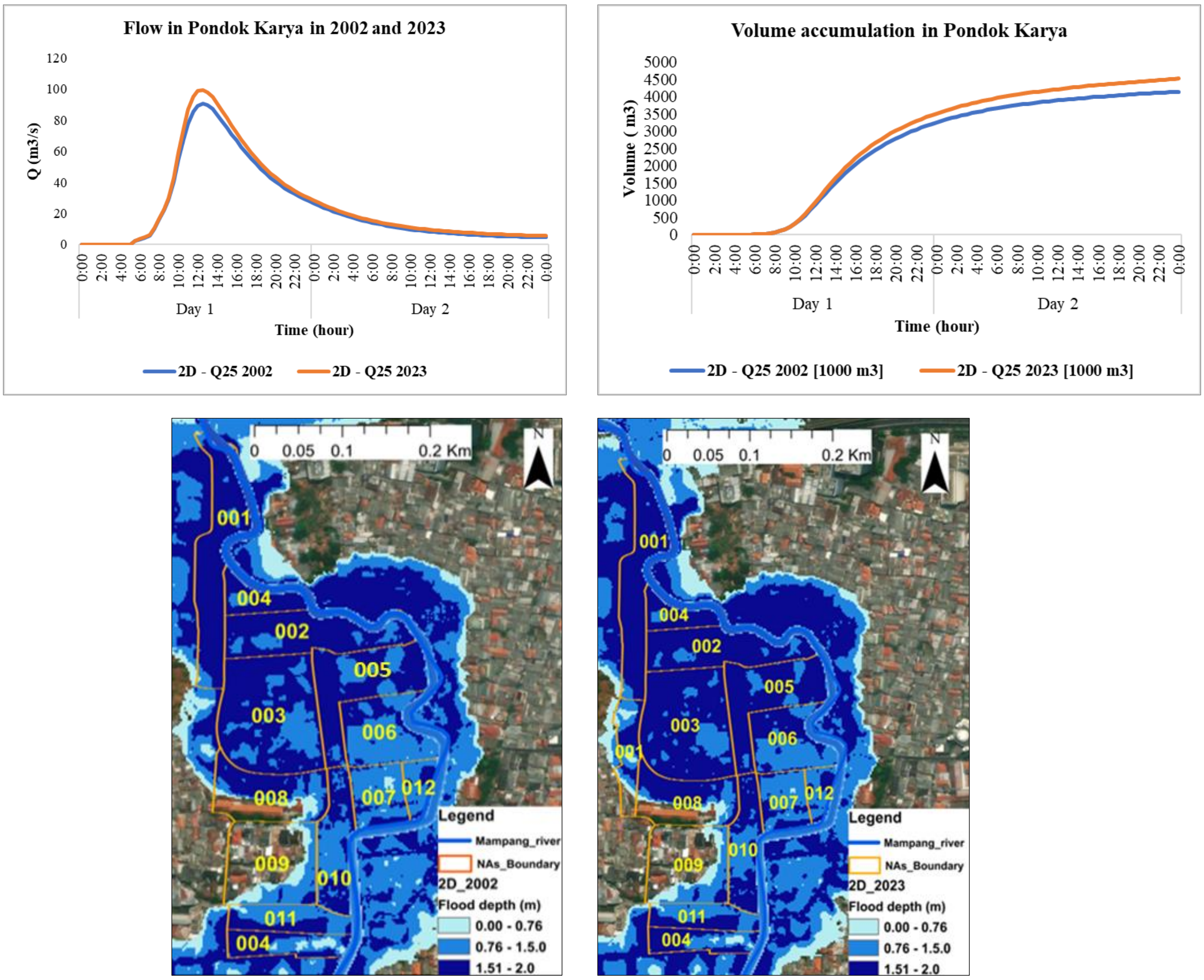

Figure 12. Flow hydrograph, volume accumulation, and the 2D flood map over Pondok Karya NAs in 2002 (Left) and 2023 (right) for Q25

Based on the results of the 1D model, the Pondok Karya stretch will exhibit a maximum flood flow of 94 m³/s in 2002 and 101 m³/s in 2023. Consequently, the flow rate increased by approximately 9 m³/s (10%) during the development period of approximately 20 years. Conversely, the stage elevation increases by approximately 10 cm in 2023. Thus, the Pondok Karya region is marginally more inundated in 2023 than in 2002. Based on cross-sectional profile data, flooding in Pondok Karya was attributed to the embankment in the upstream part of the Mampang River overflow, particularly near the Pondok Jaya Pumping Station. Overtopping of the embankment in Pondok Karya was not observed because of its height of approximately 5 m.

According to the findings of the 2D hydraulic model, the flow hydrograph of the Mampang River revealed that the peak flood in Pondok Karya will increase by approximately 10% by 2023, with the stage height rising by nearly 10 cm. The Pondok Karya neighborhood experienced flooding with water levels ranging from 0.6 to 1.5 m, plausibly originating from the upstream vicinity of Pondok Karya. The regional flood pattern appeared to be largely consistent between 2002 and 2023; this condition could be due to the area's basin-shaped topography. However, if the terrain of an affected area is flat, changes in land use in the upstream area might have a significant effect on the extent of flooding in the affected downstream area.

3.7. Model Calibration and Verification

Calibration of the model is critical; without these processes, the model cannot be used to analyze flood hazard indices. The model was calibrated by comparing the depth of flooding calculated using the HEC-RAS 1D hydraulic model with historical flood event data from 2020 to 2024 in the Pondok Karya area. Calibration was performed by using the NSE approach. Where is the outcome of the NSE computation?

As shown in Table 4, the result of calibrating the 1D hydraulic model across 10 events had an NSE value of 0.65, indicating that the model performed well, as demonstrated by the NSE criterion in Table 1. In addition to data calibration, we conducted field surveys and interviews with Pondok Karya inhabitants to cross-check data on flood heights and inundation areas of model findings with actual conditions. Many factors influenced the model calibration results, including social behavior interventions such as garbage disposal into the river, wastewater intake into the river, sedimentation, and the operation of water gates in the river, which were not included in the model simulation (Figure 13). In addition, the model assumptions and justifications owing to a lack of data contributed to the model results. In this scenario, the model was used to generate the Pondok Karya flood hazard index.

Figure 13. Verification model results with field survei and interviews with local resident in Pondok Karya Area

Table 4. Calibration results of hydraulic model 1D Pondok Karya

Flood events	**Flood depth (cm)**		**$(H_{sim}\text{-}H_{obs})^2$**	**$(H_{obs}\text{-}H_{avg})^2$**
	Simulated (H_{sim})	**Observed (H_{obs})**		
1/1/2020	163	150	169	53.50
2/19/2021	121	100	441	12.25
2/21/2021	145	150	25	53.50
11/7/2021	90	70	400	702.25
7/16/2022	65	50	225	2162.25
10/4/2022	161	150	121	150.00
10/7/2022	95	85	100	132.25
11/28/2022	75	50	625	2162.25
12/23/2022	90	100	100	100.00
3/2/2024	75	60	225	1332.25
AVERAGE		**96.50**		
SUM			**2431**	**6860.50**
			NSE	**0.65**

The lack of field data on actual land use, cross section, solid waste, and sedimentation rate may influence the reliability of the analysis of the flood hydrograph, river capacity, and inundation depth. Future research should consider the possibility of Neural Network applications to solve this problem [31, 42, 51].

3.8. Flood Hazards Index

The flood hazard index in Pondok Karya was determined by quantifying the number of Neighbourhood Associations (NAs) present, totaling 14 identified NA locations. This analysis was based on a hydraulic simulation conducted on both 1D and 2D models, followed by calibration. Hazard index analysis was performed for two distinct scenarios: 2002 and 2023. In 2002, the area of flooding was assigned a score of 0.6 due to all the NAs having a total inundation area greater than 300 m^2, categorizing its flood hazard level as high. Furthermore, this condition is projected to be applicable in 2023, as indicated by the flood map model shown in Figure 14. The flood duration was determined by conducting time-step simulations and recording field data. This encompassed the period from when flooding began to when it reached its lowest level. The dynamic value of the river is influenced by both the surface elevation and distance from the river. The analysis revealed a flooding period of 12–24 h, indicating a moderate flood concentration. The frequency of flooding was derived from the actual data series recorded by the DSDA Jakarta between 2016 and 2021, indicating inundation of more than five times each year in Pondok Karya. Consequently, a typical value of 0.6 was established for the years 2002 and 2023 for all missing values.

Figure 14. Buildings map along Mampang river

The final parameter in the flood hazard index was inundation depth, which was determined from the maximum flood depth extracted from the 2D HEC-RAS hydraulic model. The data was categorized into three groups based on their size: less than 0.76 m, 0.76–1.5 m, and more than 1.5 m, to satisfy the criteria specified in Table 1. Subsequently, the assigned value for each missing data point is established by calculating the average value of all missing data points.

The flood hazard level classifications revealed the following results: high hazard levels were identified in 42.85% (six NAs) of the area, with an equal proportion classified as moderate (42.85%, six NAs), and the remaining 14.29% (two NAs) were classified as low. However, in 2023, a notable shift occurs, with the proportion of areas classified as high increasing to 57.14% (eight NAs). Conversely, there was a decrease in areas classified as moderate, declining to 35.71% (five NAs), and those classified as low, declining to 7.14% (one NAs).

Pondok Karya is situated in a zone with high susceptibility to floods. Analysis revealed that despite over 30% plant cover in the overall catchment area of Pondok Karya in 2002, the area experienced complete inundation with water levels ranging from 0.76 m to over 1.5 m. This suggests that the Mampang River has a limited capacity and requires additional retarding basins along its upper course. Consequently, the flood hazard index is projected to increase further by 2023 (Figure 15).

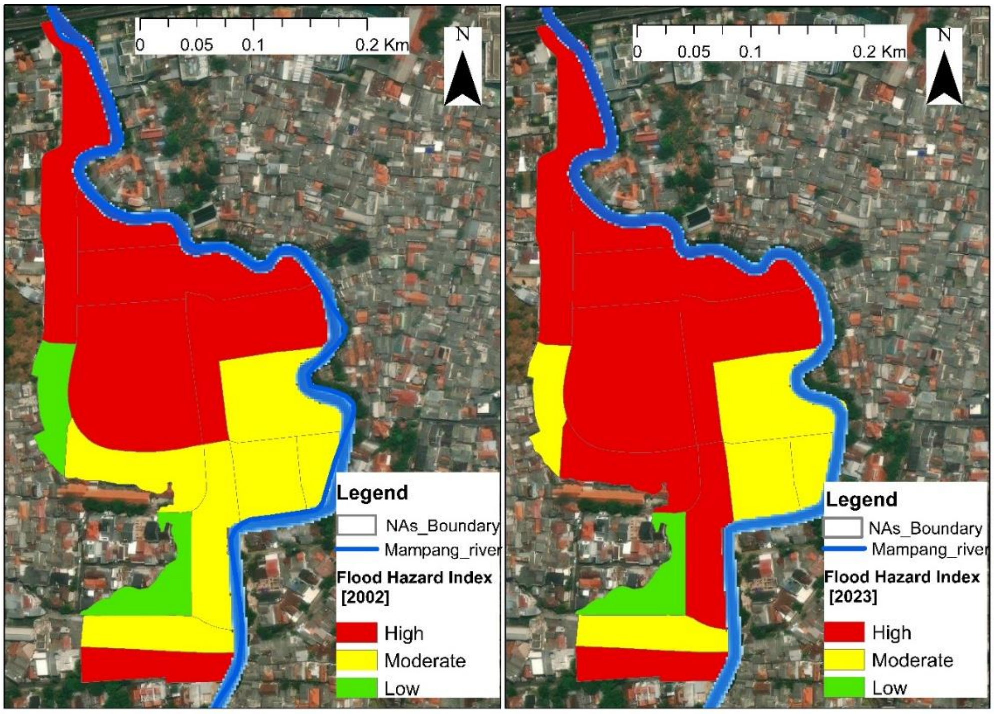

Figure 15. Flood hazard index map for Q25 in 2002 (left) and 2023 (right)

The alteration of land use and cover between 2002 and 2023 is closely linked to the occurrence of peak flood events in the Mampang River during the Q25 period. The curve number (CN) values primarily increased in the higher section of the Pondok Karya catchment region. As a result, there was an increase in surface runoff in the highland sub-basin (Table 3 and Figure 11). The soil characteristics at this location affect the rates of surface runoff and infiltration. This scenario subsequently contributes to the degree of flood threat in the Pondok Karya area.

The most comparable previous research is that of Taufik et al. (2022), who investigated flood hazards in the Bendungan Hilir village. Based on that study, the flood hazard study was conducted on a sub-district scale; however, this study was conducted at the neighborhood level, which is more thorough. The results of the previous study were lower than those of this study, which could be attributed to the fact that the previous study did not account for changes in land use and cover. However, the findings of this study indicate that the downstream areas face a high flood risk, which is consistent with the findings of this study.

4. Conclusion

The analysis revealed significant shifts in the land use change of the Pondok Karya catchment area between 2002 and 2023. Urban areas witnessed a substantial increase of 30%, vegetation cover showed a marked decline of 24%, bare land decreased by 9%, and water bodies had a small increase of 3% throughout this period. Overall, the accuracy of the land use change analysis was 80.71%, which is acceptable. Through the assessment of hydrology and hydraulics, changes in land use were found to contribute to increased surface runoff and stream flow. In 2023, a 10% increase was observed in the peak stream discharge, approximately 9 m^3/s, and the depth of flooding increases by approximately 10 cm compared to 2002 in the Pondok Karya segment. Consequently, the FHI in Pondok Karya increased from 2002 to 2023. The high hazard level increased by 14.29%, the moderate hazard level decreased by 7.14%, and the low hazard level decreased by 7.15%, respectively. Pondok Karya, located downstream of the Mampang sub-watershed, exhibited a significant flood hazard index. Notably, in the 2002 scenario, the area was completely submerged in response to Q25. The flood hazard index is projected to increase significantly by 2023. This indicates that the current capacity of the Mampang River does not yet meet the desired design, despite having a vegetation percentage of over 30% in the total catchment area of the Mampang sub-watershed. Hence, it is essential to address in the near future study an appropriate NbS flood hazard mitigation scheme for controlling the allowable future land use change. To enhance further research, updating hydraulic data, including geometric data, is crucial for developing a robust model capable of accurately predicting floods under various scenarios, either in flood risk or flood early warning systems.

5. Declarations

5.1. Author Contributions

Conceptualization, M.S.B.K., M.S., M.C., and A.A.K.; methodology, M.S., M.S.B.K., M.C., and A.A.K.; software, M.S.; validation, M.S.B.K., M.C., and A.A.K.; formal analysis, M.S.; investigation, M.S.; resources, M.S. and M.S.B.K.; data curation, M.S.; writing—original draft preparation, M.S.; writing—review and editing, M.S., M.S.B.K., M.C., and A.A.K.; visualization, M.S. and M.S.B.K.; supervision, M.S.B.K., M.C., and A.A.K.; project administration, M.S. and M.S.B.K.; funding acquisition, M.S. All authors have read and agreed to the published version of the manuscript.

5.2. Data Availability Statement

The data presented in this study are available in the article.

5.3. Funding

The authors received no financial support for the research, authorship, and/or publication of this article.

5.4. Conflicts of Interest

The authors declare no conflict of interest.

6. References

[1] Wijayanti, P., Zhu, X., Hellegers, P., Budiyono, Y., & van Ierland, E. C. (2017). Estimation of river flood damages in Jakarta, Indonesia. Natural Hazards, 86(3), 1059–1079. doi:10.1007/s11069-016-2730-1.

[2] Budiyono, Y., Aerts, J. C. J. H., Tollenaar, D., & Ward, P. J. (2016). River flood risk in Jakarta under scenarios of future change. Natural Hazards and Earth System Sciences, 16(3), 757–774. doi:10.5194/nhess-16-757-2016.

[3] Mishra, B. K., Rafiei Emam, A., Masago, Y., Kumar, P., Regmi, R. K., & Fukushi, K. (2018). Assessment of future flood inundations under climate and land use change scenarios in the Ciliwung River Basin, Jakarta. Journal of Flood Risk Management, 11, S1105–S1115. doi:10.1111/jfr3.12311.

[4] Akter, T., Quevauviller, P., Eisenreich, S. J., & Vaes, G. (2018). Impacts of climate and land use changes on flood risk management for the Schijn River, Belgium. Environmental Science and Policy, 89(July), 163–175. doi:10.1016/j.envsci.2018.07.002.

[5] Rahman, M., Ningsheng, C., Mahmud, G. I., Islam, M. M., Pourghasemi, H. R., Ahmad, H., Habumugisha, J. M., Washakh, R. M. A., Alam, M., Liu, E., Han, Z., Ni, H., Shufeng, T., & Dewan, A. (2021). Flooding and its relationship with land cover change, population growth, and road density. Geoscience Frontiers, 12(6), 101224. doi:10.1016/j.gsf.2021.101224.

[6] Kuntoro, A. A., Cahyono, M., & Soentoro, E. A. (2018). Land cover and climate change impact on river discharge: Case study of upper citarum river basin. Journal of Engineering and Technological Sciences, 50(3), 364–381. doi:10.5614/j.eng.technol.sci.2018.50.3.4.

[7] Kuntoro, A. A., Putro, A. W., Kusuma, M. S. B., & Natasaputra, S. (2017). The effect of land use change to maximum and minimum discharge in Cikapundung River Basin. AIP Conference Proceedings, 1903(November 2017). doi:10.1063/1.5011621.

[8] Sugianto, S., Deli, A., Miswar, E., Rusdi, M., & Irham, M. (2022). The Effect of Land Use and Land Cover Changes on Flood Occurrence in Teunom Watershed, Aceh Jaya. Land, 11(8). doi:10.3390/land11081271.

[9] Banjara, M., Bhusal, A., Ghimire, A. B., & Kalra, A. (2024). Impact of Land Use and Land Cover Change on Hydrological Processes in Urban Watersheds: Analysis and Forecasting for Flood Risk Management. Geosciences (Switzerland), 14(2), 40. doi:10.3390/geosciences14020040.

[10] Hosseinzadehtalaei, P., Ishadi, N. K., Tabari, H., & Willems, P. (2021). Climate change impact assessment on pluvial flooding using a distribution-based bias correction of regional climate model simulations. Journal of Hydrology, 598(December), 126239. doi:10.1016/j.jhydrol.2021.126239.

[11] Allegri, E., Zanetti, M., Torresan, S., & Critto, A. (2024). Pluvial flood risk assessment for 2021–2050 under climate change scenarios in the Metropolitan City of Venice. Science of the Total Environment, 914. doi:10.1016/j.scitotenv.2024.169925.

[12] Hamed Fahmy, A., Amin Abdelfatah, M., & El-Fiky, G. (2023). Investigating land use land cover changes and their effects on land surface temperature and urban heat islands in Sharqiyah Governorate, Egypt. Egyptian Journal of Remote Sensing and Space Science, 26(2), 293–306. doi:10.1016/j.ejrs.2023.04.001.

[13] Silva, J. S., Silva, R. M. da, & Santos, C. A. G. (2018). Spatiotemporal impact of land use/land cover changes on urban heat islands: A case study of Paço do Lumiar, Brazil. Building and Environment, 136(January), 279–292. doi:10.1016/j.buildenv.2018.03.041.

[14] Otto, F. E. L., Zachariah, M., Saeed, F., Siddiqi, A., Kamil, S., Mushtaq, H., Arulalan, T., AchutaRao, K., Chaithra, S. T., Barnes, C., Philip, S., Kew, S., Vautard, R., Koren, G., Pinto, I., Wolski, P., Vahlberg, M., Singh, R., Arrighi, J., … Clarke, B. (2023). Climate change increased extreme monsoon rainfall, flooding highly vulnerable communities in Pakistan. Environmental Research: Climate, 2(2), 025001. doi:10.1088/2752-5295/acbfd5.

[15] Tollan, A. (2002). Land-use change and floods: What do we need most, research or management? Water Science and Technology 45(8), 183–190. doi:10.2166/wst.2002.0176.

[16] Varis, O., Taka, M., & Tortajada, C. (2022). Global human exposure to urban riverine floods and storms. River, 1(1), 80–90. doi:10.1002/rvr2.1.

[17] Adnan, M. S. G., Abdullah, A. Y. M., Dewan, A., & Hall, J. W. (2020). The effects of changing land use and flood hazard on poverty in coastal Bangladesh. Land Use Policy, 99(July), 104868. doi:10.1016/j.landusepol.2020.104868.

[18] Dewi, R. P., Khofianida, A., Agista, D. E., Arrasyid, F. P., Kurniawati, Damayanti, S. I., & Putri, R. F. (2020). Landuse change in Jakarta Province: Trend, types, and socio-demographic factors. IOP Conference Series: Earth and Environmental Science, 451(1). doi:10.1088/1755-1315/451/1/012055.

[19] Rachma, T. R. N., Silalahi, F. E. S., & Oktaviani, N. (2022). Monitoring 20 Years of Land Cover Change Dynamics in the Satellite Cities of Jakarta, Indonesia. IOP Conference Series: Earth and Environmental Science, 1111(1), 012034. doi:10.1088/1755-1315/1111/1/012034.

[20] Yosua, H., Kusuma, M. S. B., & Nugroho, J. (2023). An assessment of pluvial hazard in South Jakarta based on land-use/cover change from 2016 to 2022. Frontiers in Built Environment, 9, 1–8. doi:10.3389/fbuil.2023.1345894.

[21] Babí Almenar, J., Elliot, T., Rugani, B., Philippe, B., Navarrete Gutierrez, T., Sonnemann, G., & Geneletti, D. (2021). Nexus between nature-based solutions, ecosystem services and urban challenges. Land Use Policy, 100. doi:10.1016/j.landusepol.2020.104898.

[22] Priyambodoho, B. A., Kure, S., Yagi, R., & Januriyadi, N. F. (2021). Flood inundation simulations based on GSMAP satellite rainfall data in Jakarta, Indonesia. Progress in Earth and Planetary Science, 8(1). doi:10.1186/s40645-021-00425-8.

[23] Hamel, P., & Tan, L. (2022). Blue–Green Infrastructure for Flood and Water Quality Management in Southeast Asia: Evidence and Knowledge Gaps. Environmental Management, 69(4), 699–718. doi:10.1007/s00267-021-01467-w.

[24] Christiana, D. W. (2023). Building Resilience through Nature-based Solutions: Exploring the Urban-Rural Linkages in Flood Mitigation Strategies for Jayapura. Smart City, 3(2). doi:10.56940/sc.v3.i2.3.

[25] Taufik, S. R., Yatrib, M., Harman, A. N., Kesuma, T. N. A., Saputra, D., & Kusuma, M. S. B. (2022). Assessment of flood hazard reduction in DKI Jakarta: Bendungan Hilir Village. IOP Conference Series: Earth and Environmental Science, 989(1). doi:10.1088/1755-1315/989/1/012018.

[26] Supratman, M., Kusuma, M. S. B., Cahyono, M., & Kuntoro, A. A. (2024). Flood risk assessment of Kemang Area as a central business in South Jakarta. E3S Web of Conferences, 479. doi:10.1051/e3sconf/202447903003.

[27] Farid, M., Harumi Pusparani, H., Syahril Badri Kusuma, M., & Natasaputra, S. (2017). Study on effectiveness of flood control based on risk level: Case study of Kampung Melayu Village and Bukit Duri Village. MATEC Web of Conferences, 101. doi:10.1051/matecconf/201710105003.

[28] Alves Beloqui, A. (2020). Combining Green-Blue-Grey Infrastructure for Flood Mitigation and Enhancement of Co-Benefits. CRC Press, London, United Kingdom. doi:10.1201/9781003041818.

[29] Reu Junqueira, J., Serrao-Neumann, S., & White, I. (2022). Using green infrastructure as a social equity approach to reduce flood risks and address climate change impacts: A comparison of performance between cities and towns. Cities, 131, 104051. doi:10.1016/j.cities.2022.104051.

[30] Seo, M., Jaber, F., & Srinivasan, R. (2017). Evaluating various low-impact development scenarios for optimal design criteria development. Water (Switzerland), 9(4), 270. doi:10.3390/w9040270.

[31] Enung, Kusuma, M. S. B., Kardhana, H., Suryadi, Y., & Rohmat, F. I. W. (2022). Hourly Discharge Prediction Using Long Short-Term Memory Recurrent Neural Network (Lstm-Rnn) in the Upper Citarum River. International Journal of GEOMATE, 23(98), 147–154. doi:10.21660/2022.98.3462.

[32] Bennett, W. G., Karunarathna, H., Xuan, Y., Kusuma, M. S. B., Farid, M., Kuntoro, A. A., Rahayu, H. P., Kombaitan, B., Septiadi, D., Kesuma, T. N. A., Haigh, R., & Amaratunga, D. (2023). Modelling compound flooding: a case study from Jakarta, Indonesia. Natural Hazards, 118(1), 277–305. doi:10.1007/s11069-023-06001-1.

[33] Formánek, A., Silasari, R., Kusuma, M. S. B., & Kardhana, H. (2013). Two-dimensional model of ciliwung river flood in DKI Jakarta for development of the regional flood index map. Journal of Engineering and Technological Sciences, 45(3), 307–325. doi:10.5614/j.eng.technol.sci.2013.45.3.7.

[34] Pratiwi, V., Badri Kusuma, M. S., Kardhana, H., & Farid, M. (2020). Experimental Study of Dam Break Flow Generated By the Flap Gate in Horizontal Channel. International Journal of GEOMATE, 19(75), 19–26. doi:10.21660/2020.75.16098.

[35] Isma, F., Kusuma, M. S. B., Nugroho, E. O., & Adityawan, M. B. (2024). Flood hazard assessment in Kuala Langsa village, Langsa city, Aceh Province-Indonesia. Case Studies in Chemical and Environmental Engineering, 10, 100861. doi:10.1016/j.cscee.2024.100861.

[36] Yatsrib, M., Harman, A. N., Taufik, S. R., Kesuma, T. N. A., Saputra, D., Kusuma, M. S. B., Farid, M., & Kuntoro, A. A. (2021). Study on the Contribution of Normalization to Reducing Flood Risk in the Ciliwung River, Tebet District, Jakarta. IOP Conference Series: Earth and Environmental Science, 933(1), 012032. doi:10.1088/1755-1315/933/1/012032.

[37] Rizaldi, A., Badri Kusuma, M. S., Kuntoro, A. A., & Kardhana, H. (2022). Trend Analysis of Rainfall, Land Cover, and Flow Discharge in the Citarum Hulu–Majalaya Basin. International Journal on Advanced Science, Engineering and Information Technology, 12(4), 1469. doi:10.18517/ijaseit.12.4.15225.

[38] Kesuma, T. N. A., Kusuma, M. S. B., Farid, M., Kuntoro, A. A., & Rahayu, H. P. (2022). An Assessment of Flood Hazards Due To the Breach of the Manggarai Flood Gate. International Journal of GEOMATE, 23(95), 104–111. doi:10.21660/2022.95.3055.

[39] Juliana, I. C., Kusuma, M. S. B., Cahyono, M., Martokusumo, W., & Kuntoro, A. A. (2017). The effect of differences rainfall data duration and time period in the assessment of rainwater harvesting system performance for domestic water use. AIP Conference Proceedings, 1903. doi:10.1063/1.5011616.

[40] Suprapti, S., Kusuma, M. S. B., Kardhana, H., & Cahyono, M. (2024). An assessment of potential infiltration areas to support groundwater supply system in Jagakarsa, South Jakarta, based on Multi-Criteria Decision-Making (MCDM) analysis. Case Studies in Chemical and Environmental Engineering, 10, 100799. doi:10.1016/j.cscee.2024.100799.

[41] Kusuma, M. S. B., Setiawati, T., & Farid, M. (2019). Experimental model of dam break flow around several blockages configurations. International Journal of GEOMATE, 16(58), 26–32. doi:10.21660/2019.58.97684.

[42] Kardhana, H., Valerian, J. R., Rohmat, F. I. W., & Kusuma, M. S. B. (2022). Improving Jakarta's Katulampa Barrage Extreme Water Level Prediction Using Satellite-Based Long Short-Term Memory (LSTM) Neural Networks. Water (Switzerland), 14(9), 1469. doi:10.3390/w14091469.

[43] Kusuma, M. S. B., Ragayu, R. A., & Cahyono, M. (2009). Development study of turbulent κ-ε model for recirculation flow III: Two-dimension recirculation flow in a reservoir. ITB Journal of Engineering Science, 41(1), 1–16. doi:10.5614/itbj.eng.sci.2009.41.1.1.

[44] Sengara, W., Latief, H., Syahril, M., & Kusuma, B. (2008). Geotechnical Engineering for Disaster Mitigation and Rehabilitation. Geotechnical Engineering for Disaster Mitigation and Rehabilitation. Springer, Berlin, Germany. doi:10.1007/978-3-540-79846-0.

[45] Abdessamed, D., & Abderrazak, B. (2019). Coupling HEC-RAS and HEC-HMS in rainfall–runoff modeling and evaluating floodplain inundation maps in arid environments: case study of Ain Sefra city, Ksour Mountain. SW of Algeria. Environmental Earth Sciences, 78(19). doi:10.1007/s12665-019-8604-6.

[46] Thakur, B., Parajuli, R., Kalra, A., Ahmad, S., & Gupta, R. (2017). Coupling HEC-RAS and HEC-HMS in Precipitation Runoff Modelling and Evaluating Flood Plain Inundation Map. World Environmental and Water Resources Congress 2017, 240–251. doi:10.1061/9780784480625.022.

[47] Peker, İ. B., Gülbaz, S., Demir, V., Orhan, O., & Beden, N. (2024). Integration of HEC-RAS and HEC-HMS with GIS in Flood Modeling and Flood Hazard Mapping. Sustainability (Switzerland), 16(3), 1226. doi:10.3390/su16031226.

[48] Sisodia, P. S., Tiwari, V., & Kumar, A. (2014). Analysis of Supervised Maximum Likelihood Classification for remote sensing image. International Conference on Recent Advances and Innovations in Engineering (ICRAIE-2014), Jaipur, India. doi:10.1109/icraie.2014.6909319.

[49] Arifin, S. (2015). Study of Standard Components and Criteria for Digital Processing of Multispectral Remote Sensing Data for Land Cover Classification. Prosiding Pertemuan Ilmiah Tahunan XX dan Kongres VI Masyarakat Ahli Penginderaan Jauh Indonesia (MAPIN), 5-6 February, 2015, Darmaga Bogor, Indonesia.

[50] Saputra, N. E., Wibowo, C., & Lisnawati, Y. (2021). Analysis of soil physical properties and infiltration rates for various landuses at Gunung Dahu Research Forest, Bogor District, West Java Province. IOP Conference Series: Earth and Environmental Science, 713(1), 012034. doi:10.1088/1755-1315/713/1/012034.

[51] Ari Gunawan, T., Syahril Badri Kusuma, M., Cahyono, M., & Nugroho, J. (2017). The application of backpropagation neural network method to estimate the sediment loads. MATEC Web of Conferences, 101. doi:10.1051/matecconf/201710105016.